Experimental validation of an hybrid analytical-numerical technique to estimate the directivity of ultrasonic piezoelectric actuators

Emanuele De Bono, Manuel Collet, Jerome Grando, Kerem Ege

25·29 August 2024
inter.noise
NANTES FRANCE

Experimental validation of an hybrid analytical-numerical technique to estimate the directivity of ultrasonic piezoelectric actuators

Emanuele De Bono[1]
Laboratoire de Tribologie et Dynamique des Systèmes (LTDS), École Centrale de Lyon (ECL)
36 Av. Guy de Collongue, 69134 Écully

Manuel Collet[2]
Laboratoire de Tribologie et Dynamique des Systèmes (LTDS), École Centrale de Lyon (ECL)
36 Av. Guy de Collongue, 69134 Écully

Jerome Grando[3]
Plastic Omnium
19 Bd Jules Carteret, 69007 Lyon, France

Kerem Ege[4]
Laboratoire Vibrations Acoustique
INSA Lyon, LVA, UR677, 69621 Villeurbanne, France

ABSTRACT

The generation of guided waves is a common approach for the interrogation of the state of health of structural components. The optimization of the excitation strategies very much benefits from the availability of efficient simulation tools, which are capable of accurately predicting the propagation of waves generated through various sources, and their interaction with damage or structural defects. On the one hand, the application of finite elements (FEs) for the analysis of wave propagation problems leads to large models which tend to be computationally costly for parametric or optimization studies. On the other hand, semi-analytical approaches for wave propagation analysis provide useful analytical expressions for conducting parametric studies, but may lead to inaccurate estimations of tuning frequencies and directionality, especially at high frequencies. This is mostly because of the simplifying assumptions regarding the stress field at the interface between the actuator patches and the plate. A methodology was proposed which couples the analytical far-field solution of the plate response with a local FE model of the interaction between the plate and the patch, through which the interface stresses are numerically estimated. The local FE model of the electro-mechanical behaviour of the plate/patch system allows the analysis of complex actuation configurations for optimal tuning, directivity steering and focusing strategies. In this contribution, we experimentally validate such hybrid FE-analytical technique. A Scanning

[1]emanueledeb88@hotmail.it

[2]manuel.collet@ec-lyon.fr

[3]jerome.grando@plasticomnium.com

[4]kerem.ege@insa-lyon.fr

Laser Doppler velocimeter is employed to retrieve both temporal and spatial Fourier Transforms on a polycarbonate plate, excited by piezoelectric patches, and the directivity patterns of the first symmetric and antisymmetric modes are compared to the numerical predictions.

1. INTRODUCTION

Of particular importance is the estimation of guided waves generated by surface mounted or embedded piezoelectric patches or wafer transducers, for which accurate models are essential tools for the selection of geometry, dimensions, and excitation bandwidth suitable for the excitation of specific modes and the detection of various damage types. A common methodology is based on the solution of the wave equation in the spatial Fourier domain. This technique has been applied to the analysis of waves generated by several actuator configurations in isotropic structures. These results, which are limited to one-dimensional (1D) wave propagation, are extended to the 2D analysis of wave propagation in plates in [1], where an analytical model allows the investigation of the effects of the in-plane shape of the piezo patch. The formulation of [1] relies on the solution of the 3D equations of elasticity with the stress field generated by the surface bonded piezo as a boundary condition. The analytical derivations assume simplified expressions for such stress distributions, which allows the analytical derivations of the plate response. The obtained analytical expressions are very useful for conducting parametric studies and for the convenient interpretation of experimental measurements, but may lead to inaccurate estimations of tuning frequencies and directionality, specifically at high frequencies. In particular, the assumption that piezoelectric stresses are concentrated on the boundaries of the patch leads to neglecting the shear lag phenomena associated with the presence of a bonding layer [2], which results in the inaccurate estimation of the tuning conditions for the actuation [3]. In [4], the analytical far field solution of the plate response is coupled with a local FE model of the interaction between the plate and the patch, through which the interface stresses are numerically estimated. The local FE model of the electro-mechanical behaviour of the plate/patch system allows the analysis of complex actuation configurations, and the possibility of including bonding conditions. In this contribution, we experimentally validate such hybrid FE-analytical technique, by measuring the directivity patterns of the first symmetric and antisymmetric modes.

2. NUMERICAL SIMULATIONS FOR THE DIRECTIVITY

The directivity pattern of the shear field produced by the piezoelectric actuator can be estimated through the spatial Fourier Transform of the static stresses realized at the interface between plate and piezoelectric actuator, according to the methodology proposed by Collet et al. in [4]. So, first step is to solve the static problem for the shear stress at the interface between piezoelectric patch and plate. We are now dealing with the 3D system.

2.1. Single rectangular patch

In Figure 1, the traction forces $T_{ax}(x,y)$, $T_{ay}(x,y)$ applied on the interface between patch and plate are displayed. The plate guided modes and corresponding wavenumbers are computed analytically. The Fourier transform of the static traction field at the interface piezo-plate are obtained by numerically solving the Fourier transform integral on the Finite Element (FE) mesh of Comsol. We have found very useful to employ the integration facility of Comsol (as suggested in [4] as well), allowing to take advantage of the shape-functions (usually Lagrange interpolators) in order to reduce numerical errors typical of Discrete-Fourier-Transform (DFT) algorithms. Nevertheless, the DFT, and especially the Fast-Fourier-Transform FFT algorithm, allows faster computation.

In Figure 2 the meshed surface employed for integration is highlighted: it is a circle with centre at

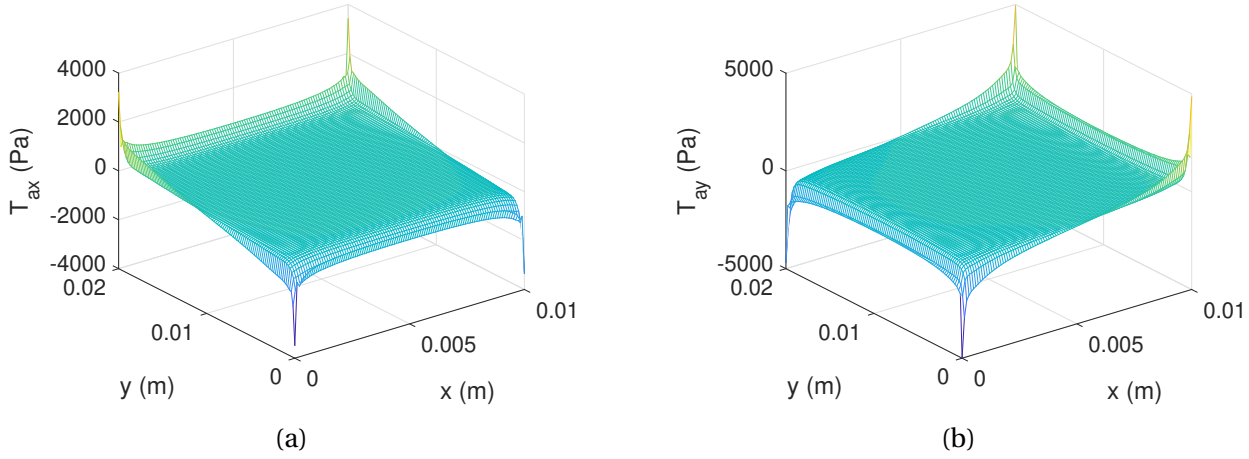

Figure 1: Static traction forces $T_{ax}(x,y)$, $T_{ay}(x,y)$ at the interface patch-plate.

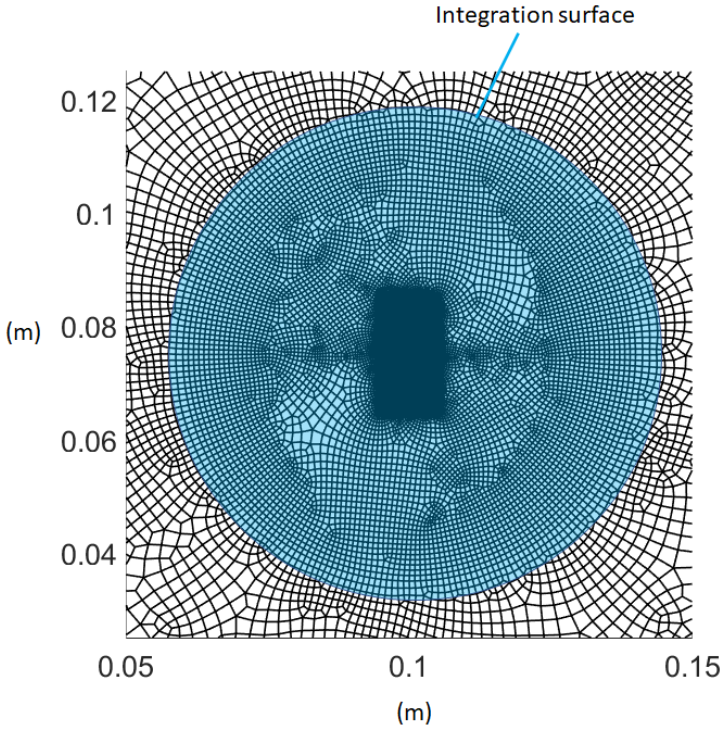

Figure 2: Surface of integration for the Fourier Transform integrals.

the piezo-patch centre of symmetry and of radius R_I twice the maximum size of the patch. The mesh adopted for such surface is such that the wavelength of mode A0 at the maximum frequency of interest, is 5 times the maximum mesh element size Δr. This minimizes the aliasing effects. The maximum frequency of interest here is 200 kHz.

The size of integration domain defines the step size of the Fourier Spatial coordinates ($\Delta\xi_R = 1/R_I$), while the maximum element size in the mesh defines the extension of the Fourier spatial domain ($\xi_{R_{max}} = 1/2\Delta r$).

From $\tilde{T}_{ax}(\xi_R,\phi)$ and $\tilde{T}_{ay}(\xi_R,\phi)$, we can obtain the Fourier Transform of the radial component $\tilde{T}_{aR}(\xi_R,\phi)$:

$$\tilde{T}_{aR}(\xi_R,\phi) = \sqrt{[\tilde{T}_{ax}(\xi_R,\phi)]^2 + [\tilde{T}_{ay}(\xi_R,\phi)]^2}. \tag{1}$$

In order to find the directivity of modes A0 and S0 (other modes could also be investigated), we need to solve the dispersion problem of the plate. The frequency response relative to the out-of-plane displacement w in the Fourier polar coordinates (ξ_R, ϕ), is given by:

$$\tilde{w}(\omega, \xi_R, \phi) = \frac{V_0(\omega)}{4\pi\mu} G_w(\omega, \xi_R) \tilde{T}_{aR}(\xi_R, \theta) \,, \tag{2}$$

where the function $G_w(\omega, \xi_R)$ multiplying $\tilde{T}_{aR}$ is the frequency response for unit traction force applied on an infinite waveguide of uniform thickness $2b$. Hence we refer to $G_w(\omega, \xi_R)$ as the Green's function of the system. By the Inverse-spatial-Fourier Transform of $\tilde{w}(\omega, \xi_R, \phi)$, we obtain the frequency response in physical coordinates $w(\omega, r, \theta)$, r and θ being the physical radius and angle respectively. The Inverse-spatial-Fourier Transform is a double integral in $d\xi_R$ and $d\phi$. To simplify such computation, in [4], the integration over the angle coordinate is approximated through the Stationary Value Theorem for large values of r (as we are interested in the far-field radiation). The solution can be obtained by a 1D FFT algorithm for assigned values of θ, as suggested in [4].

Observe that the intersection between the dispersion plot of mode m in the plane (ξ_R, ϕ) at a fixed frequency $f = \bar{f}$, and $\tilde{T}_{aR}(\xi_R, \phi)$, gives the shape of the directivity pattern of mode m at frequency $\bar{f}$, but not the actual values of it. We remind, once again, that if the plate is isotropic (as it is the case now), the dispersion plot of each mode m is independent of ϕ. In Figure 3a we have plotted, along with $\tilde{T}_{aR}(\xi_R, \theta)$, the dispersion curves of modes A0 and S0 at $\bar{f} = 100$ kHz: they are circles of equations $\xi_R = \xi_{A0}(\bar{f})$ and $\xi_R = \xi_{S0}(\bar{f})$.

The directivity patterns of modes A0 and S0 at 100 kHz are plotted in Figure 3b. Observe that for mode A0 the directivity along the x direction (perpendicular to the longest size of the patch) doubles the value along the y direction.

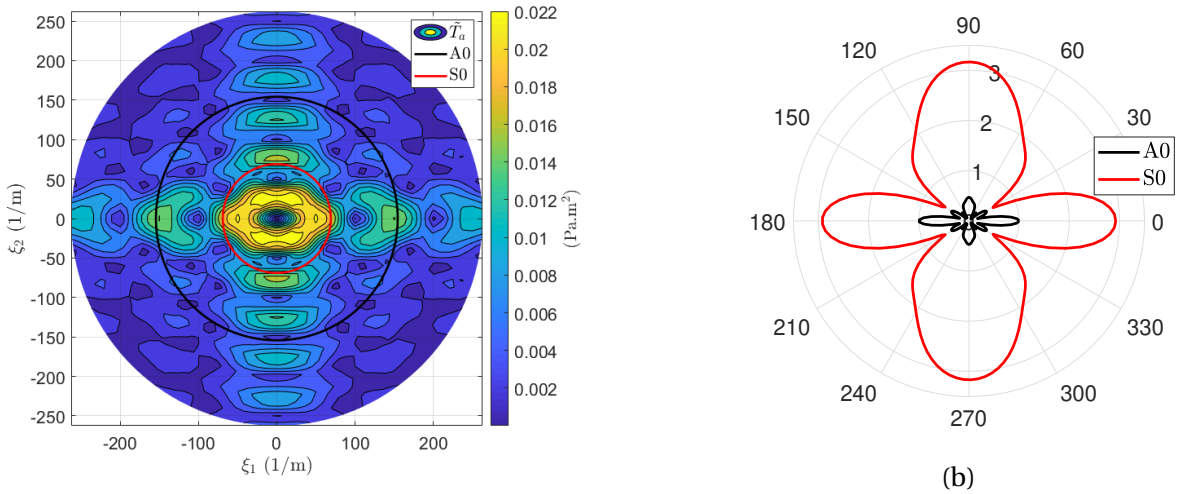

(a) (b)

Figure 3: $\tilde{T}_{aR}(\xi_R, \phi)$ and dispersion curves of modes A0 and S0 at 100 kHz **(a)** and corresponding directivity patterns **(b)**.

3. EXPERIMENTAL DISPERSION

In order to verify the accuracy of the model employed for the plate, its dispersion characteristics can be retrieved experimentally by studying the propagation of a burst signal along a plate [5]. The outcomes can also give insights about the reliability of the directivity patterns numerically predicted in Section 2.

The measurements have been conducted thanks to the Polytec Scanning (laser-Doppler) Vibrometer (PSV-400-M2-20) for high frequencies, available at the Laboratory of Vibration and Acoustics (LVA) at the INSA university in Lyon. Not all the measurement data will be presented, but just the most significant ones with low noise-to-signal ratio. Indeed, the camera and lenses of the PSV instrument presented very unstable focusing, and the signal level could easily reduce below the noise level. Considering the number of acquisitions (because of the mesh requirements for DFT of ultrasonic signals), the measurement process is very delicate and time consuming.

Both the excitation (voltage on the piezoelectric) and acquisition (velocity on the plate) are digital signals: the sampling frequency has been chosen as $f_s = 1024$ kHz, and the number of sampling $N_s = 4096$, for a total acquisition time $t_{span} = N_s/f_s = 4$ ms. If the PSV is used for generating the excitation signal (as in our case), it is necessary to define the "repeat frequency" which is nothing else that $1/t_{span}$ in our case.
The excitation signal is a Gaussian pulse, of equation

$$V(t) = V_0 \cos\Big[2\pi f_c\Big(t - 1/\Delta f\Big)\Big] e^{-[(t-\frac{1}{\Delta f})\pi\Delta f]^2}, \tag{3}$$

with V_0 the voltage amplitude, f_c and Δf the central frequency and deviation of the Gaussian bell spectrum. We have studied two types of excitations, both have $f_c = 100$ kHz, while Δf is taken first equal to 1 kHz, and then equal to 10 kHz.

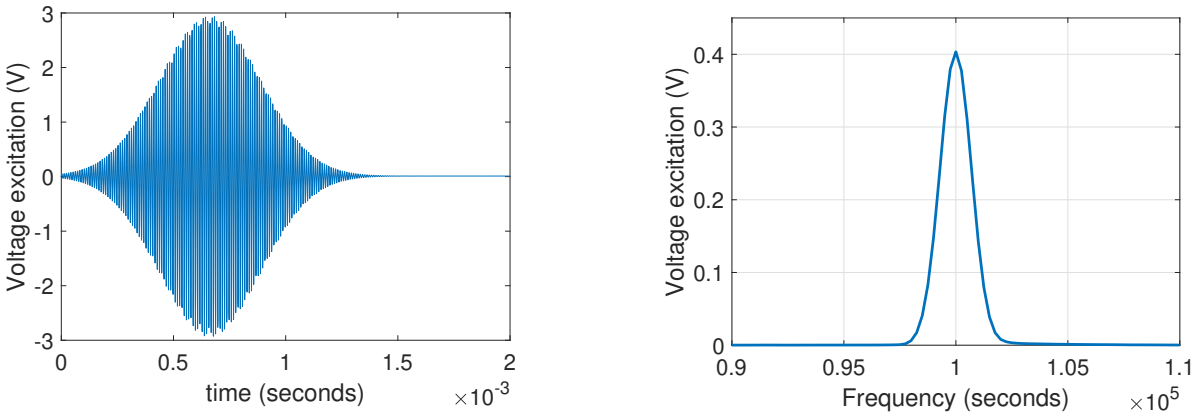

(a) (b)

Figure 4: Voltage excitation Gaussian pulse signal with $f_c = 100$ kHz and $\Delta f = 1$ kHz.

In Figure 4, the voltage excitation relative to $\Delta f = 1$ kHz is plotted in time and frequency. The piezoelectric patch of size 0.01×0.02 m has been applied on the polycarbonate plate of size 0.4×0.3 m. The measurements of out-of-plane velocity w have been carried out on a mesh defined on the first quadrant of the plate-plane with origin in the patch centre, see Figure 5. The mesh grid has 37 points along x and 33 along y, with a distance between two acquisition points $\Delta x = \Delta y \approx 0.001$ m.
An FFT both in time and space, has been applied to the acquired signals. Keeping in mind the directivity pattern of Figure 3b, it is interesting to analyse the velocity field along the two perpendicular directions x and y, corresponding to $\phi = 0$ and $\phi = 90$ degrees respectively. In Figures 7 and 6 we have plotted the time histories **(a)** along x and y directions respectively, and the corresponding Double-Fourier-Transforms **(b)** obtained by FFT algorithm, in case of Gaussian voltage excitation with $f_c = 100$ kHz and $\Delta f = 1$ kHz. The plots of the out-of-plane velocity in the Fourier Space $(f, \xi_{1/2})$ are accompanied with the dispersion curves $\xi_{1/2}(f)$ of modes A0 and S0. Notice that the mode A0 is significantly less evident along ξ_2, i.e. along the direction (y

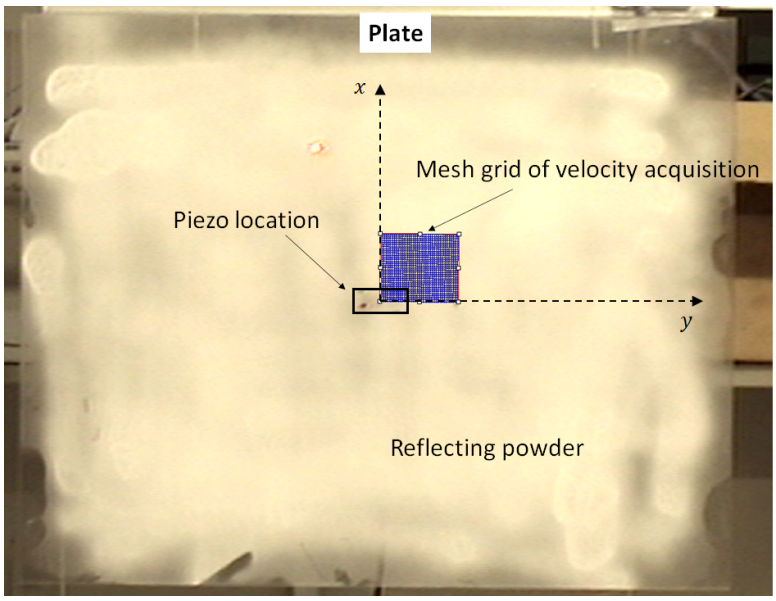

Figure 5: Mesh of acquisition points on the plate for the single piezoelectric patch.

here) parallel to the patch major size. Whereas, the mode S0 is evident both along ξ_1 and ξ_2, i.e. along both parallel and perpendicular directions with respect to the piezoelectric patch major size. This is in total agreement with the numerical results on the directivity pattern presented in Figure 3b. Indeed, in Figure 3b the numerical directivity value of mode A0 along x ($\theta = 0$ degree, corresponding to ξ_1) is two times the one along y ($\theta = 90$ degrees, corresponding to ξ_2). On the contrary, the numerical directivity of mode S0 presents approximately the same value for both directions.

A better indication about the actual directivity could be obtained by defining a circular grid in polar coordinates for the acquisition points, which would then facilitate the FFT computation to retrieve directly the out-of-plane velocity $\dot{w}(f,\xi_R,\phi)$ in Fourier polar coordinates. Also, the central frequency of voltage excitation should be varied to retrieve the above results all along the frequency range of interest.

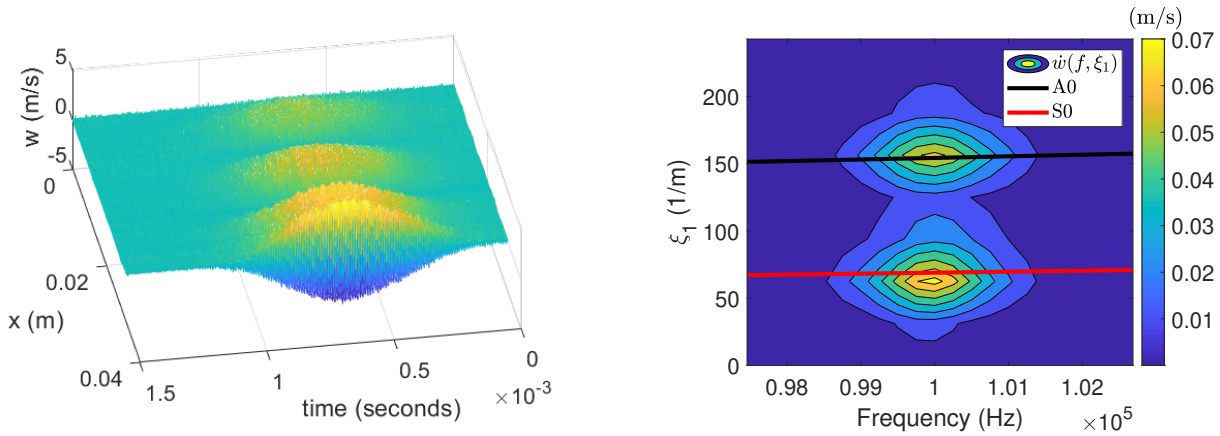

(a) (b)

Figure 6: Measured out-of-plane velocity time-histories on points along x **(a)** and corresponding Double-Fourier-Transform **(b)**, for voltage excitation Gaussian pulse with $f_c = 100$ kHz and $\Delta f = 1$ kHz.

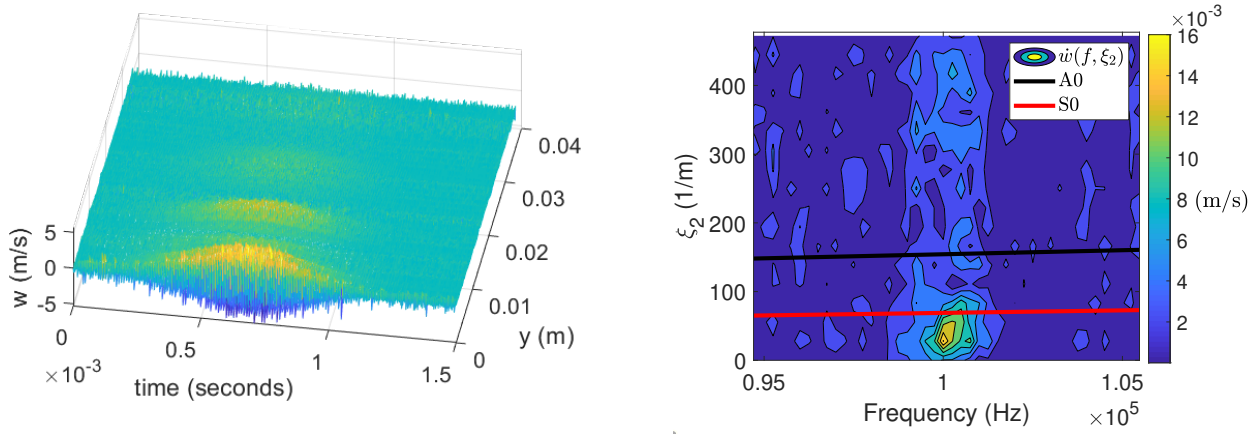

(a) (b)

Figure 7: Measured out-of-plane velocity time-histories on points along y **(a)** and corresponding Double-Fourier-Transform **(b)**, for voltage excitation Gaussian pulse with $f_c = 100$ kHz and $\Delta f = 1$ kHz.

4. CONCLUSIONS

The numerical method of [4] has been re-coded in Comsol and it has been partially validated against measurements obtained by the Polytec scanner laser-Doppler-velocimeter. The next steps consist in varying the central frequency of the Gaussian pulse signal of excitation as well as testing the rosette configuration of piezoelectric patches in *dephased* mode. The directivity of different selections of amplitudes and phases can now be easily studied thanks to the numerical tools here developed.

REFERENCES

1. Ajay Raghavan and Carlos E S Cesnik. Finite-dimensional piezoelectric transducer modeling for guided wave based structural health monitoring. *Smart materials and structures*, 14(6):1448, 2005.
2. Edward F Crawley and Javier De Luis. Use of piezoelectric actuators as elements of intelligent structures. *AIAA journal*, 25(10):1373–1385, 1987.
3. Francesco di Scalea and Salvatore Salamone. Temperature effects in ultrasonic Lamb wave structural health monitoring systems. *The Journal of the Acoustical Society of America*, 124(1):161–174, 2008.
4. M Collet, M Ruzzene, and K A Cunefare. Generation of Lamb waves through surface mounted macro-fiber composite transducers. *Smart Materials and Structures*, 20(2):25020, 2011.
5. D Alleyne and Peter Cawley. A two-dimensional Fourier transform method for the measurement of propagating multimode signals. *The Journal of the Acoustical Society of America*, 89(3):1159–1168, 1991.